9-30-1994

Blur Identification Based on Higher Order Spectral Nulls

Andreas Savakis
University of Rochester

Roger L. Easton
Rochester Institute of Technology

BLUR IDENTIFICATION BASED ON HIGHER ORDER SPECTRAL NULLS

Andreas E. Savakis* and Roger L. Easton Jr.**

* Department of Physiology, Box 642
University of Rochester Medical Center
Rochester, New York 14642

**Center for Imaging Science
Rochester Institute of Technology
Rochester, New York 14623

Abstract

The identification of the point spread function (PSF) from the degraded image data constitutes an important first step in image restoration that is known as blur identification. Though a number of blur identification algorithms have been developed in recent years, two of the earlier methods based on the power spectrum and power cepstrum remain popular, because they are easy to implement and have proved to be effective in practical situations. Both methods are limited to PSF's which exhibit spectral nulls, such as due to defocused lens and linear motion blur. Another limitation of these methods is the degradation of their performance in the presence of observation noise. The central slice of the power bispectrum has been employed as an alternative to the power spectrum which can suppress the effects of additive Gaussian noise. In this paper, we utilize the bicepstrum for the identification of linear motion and defocus blurs. We present simulation results where the performance of the blur identification methods based on the spectrum, the cepstrum, the bispectrum and the bicepstrum is compared for different blur sizes and signal-to-noise ratio levels.

1. INTRODUCTION

The estimation of the point spread function (PSF) from the degraded image is often required in image restoration and is known as blur identification. The blur identification problem has received considerable attention in recent years [1-7]. However, two of the earliest blur identification methods based on the power spectrum [8] and power cepstrum [9] are still widely used despite the development of more sophisticated algorithms. The popularity of the spectral and cepstral methods is partly due to their effectiveness when dealing with certain types of blurs, and partly due to their simplicity which results in easy implementation.

Spectral and cepstral methods can only be used to identify PSF's which exhibit periodic or nearly periodic spectral nulls such as linear motion and out-of-focus blurs. In addition, they do not consider the observation noise explicitly. When the signal-to-noise ratio (SNR) level is low, the noise power spectrum obscures the spectral nulls of the degraded image and reduces the performance of these methods. In practice, many sections of the degraded image are averaged to reduce the effects of noise on the power spectral estimate. Blur identification using the

0-8194-1626-6/94/$6.00

bispectrum was proposed as an alternative to the power spectrum which performs better in the presence of additive Gaussian noise [10]. It was shown that the two-dimensional central slice of the bispectrum is sufficient for blur identification purposes, thus an efficient implementation was obtained.

In this paper, the bicepstrum is used for the identification of blurs which exhibit periodic nulls in the central slice of the bispectrum. The bicepstrum utilizes the bispectrum and thus inherits superior performance in the presence of additive Gaussian noise. Furthermore, it can be implemented without user intervention, since blur parameter estimation is based on the global maximum rather than a local minimum. We present simulation results where we compare the blur identification performance of the power spectrum, power cepstrum, bispectrum, and bicepstrum for different blur sizes and SNR levels.

2. BLUR IDENTIFICATION BASED ON SPECTRAL NULLS

2.1 Image and PSF Models

The degraded image is modeled using a space-invariant linear degradation model:

$$g(i,j) = h(i,j) ** f(i,j) + n(i,j) \tag{1}$$

where $**$ denotes two-dimensional convolution and $g(i,j)$, $f(i,j)$, $h(i,j)$, and $n(i,j)$ represent the original image, the point spread function, and the additive signal-independent Gaussian noise, respectively. Spectral and cepstral methods do not assume a particular model for the original image, but they require the presence of periodic or nearly periodic zeros in the power spectrum of the PSF. This condition is met by some commonly encountered blurs, such as due to uniform linear motion and out-of-focus lens. The linear motion PSF is modeled by a rectangle oriented in the direction of motion. The frequency response of the linear motion blur has the shape of a sinc function in the direction that the motion occurred. Thus, the spectral nulls of the linear motion blur are periodic. The PSF due to out-of-focus lens with circular aperture is modeled by a uniform disk. The frequency response of the out-of-focus PSF is circularly symmetric with nulls occurring at concentric circles which are nearly periodic.

2.2 The Power Spectrum

In the frequency domain, the relationship between the power spectra in (1) becomes

$$P_g(u,v) = |H(u,v)|^2 \, P_f(u,v) + P_n(u,v) \tag{2}$$

where $|H(u,v)|$ is the magnitude of the Fourier transform of the PSF, and $P_g(u,v)$, $P_f(u,v)$, and $P_n(u,v)$ are the power spectra of the degraded image, original image, and noise respectively.

Spectral methods are based on the assumptions that the noise power spectrum is negligible and the spectral nulls in the power spectrum of the degraded image are exclusively due to the PSF. In practice, the noise level is not negligible, and the PSF spectral nulls appear as local minima in the power spectrum of the degraded image. The image power typically is concentrated in the lower frequencies, while the noise power spectrum is relatively flat, thus, the SNR is considerably lower in the higher frequencies. As a result, only the first prominent local minimum is used to identify the blur parameters. Sectioning and averaging is needed to reduce the noise power spectrum. The averaged periodogram is used to obtain the power spectral estimate of the recorded image [11]:

$$P_g^{(M)}(u,v) = \frac{1}{M}\sum_{k=1}^{M}\left|G^{(k)}(u,v)\right|^2 \tag{5}$$

where M is the total number of sections which are averaged, and $G(u,v)$ is the Fourier transform of the k^{th} data section. The data is windowed to reduce the effects of the window sidelobes and data discontinuities at the edges.

2.3 The Power Cepstrum

The use of the power cepstrum for blur identification [9] is based on the presence of periodic or nearly periodic nulls in the PSF power spectrum, which result in periodic local minima in the degraded image power spectrum. The power cepstrum is defined as

$$C_g(p,q) = \mathcal{F}^{-1}\left\{\log[P_g(u,v)]\right\} \tag{6}$$

where $\mathcal{F}^{-1}\{\cdot\}$ denotes the inverse Fourier Transform operator. The logarithm of the power spectrum yields large negative spikes at the locations of the local minima of the power spectrum. The periodicity of the spikes is detected by taking the inverse Fourier transform.

Blur identification using the power cepstrum provides some advantages over the power spectrum. First, it is easy to automatically detect the global maximum in the power cepstrum, as opposed to the first prominent local minimum in the power spectrum. In addition, the power cepstrum is based on multiple spectral nulls, so that even if there is an error due to noise in the location of the first local minimum in the power spectrum, it is possible to obtain the correct PSF estimate using the power cepstrum. Finally, postprocessing may be used to enhance the power cepstrum. There are often spurious peaks in the cepstrum due to the presence of noise. At low SNR levels the spurious peaks increase and may obscure the cepstral peak due to the blur. The effects of the unwanted peaks may be reduced using the approach of [12] which takes advantage of the presence of rahmonics (cepstral domain harmonics) associated with the true cepstral peak. The quefrencies (cepstral domain frequencies) which exhibit rahmonics are enhanced because they are more likely to be due to the PSF. The quefrencies which do not have rahmonics are suppressed because they are more likely to be due to noise. Due to averaging the cepstrum is reduced to a one-dimensional signal which is processed as follows:

$$C_l(p) = \frac{C(p)}{\sqrt{\frac{1}{M}\sum_{q \in A_p} C^2(q)}}, \tag{7}$$

where M is the number of points in A_p, where A_p is the set of points where rahmonics are not expected. For quefrency p, the set A_p consists of points $\{q\colon q > p_0$ and $q \notin (kp-1,\ kp,\ kp+1),\ k = 0,1,2,\ldots\}$. The value of p_0 is taken to be 4, and a point above and below multiples of p are excluded to allow for discretization errors. The choice of A_p implies that cepstrum postprocessing cannot be used to identify small blurs.

3. BLUR IDENTIFICATION BASED ON HIGHER-ORDER SPECTRAL NULLS

3.1 The Bispectrum

Use of the bispectrum in place of the power spectrum for blur identification is motivated by the fact that the bispectrum is blind to additive Gaussian noise [13]. The bispectrum of the degraded image is:

$$B_g(u_1,v_1;u_2,v_2) = H(u_1,v_1)H(u_2,v_2)H^*(u_1+u_2,v_1+v_2)B_f(u_1,v_1;u_2,v_2) + B_n(u_1,v_1;u_2,v_2) \tag{8}$$

where $B_g(u_1,v_1;u_2,v_2)$, $B_f(u_1,v_1;u_2,v_2)$, and $B_n(u_1,v_1;u_2,v_2)$ are the bispectra of the degraded image, the original image, and noise respectively. The bispectrum is a four-dimensional function and its implementation is computationally demanding. However, the central slice of the bispectrum is sufficient for blur identification [10]:

$$B_g(u,v;0,0) = |H(u_1,v_1)|^2 H(0,0) B_f(u_1,v_1;0,0) \tag{9}$$

The central slice of the bispectrum is two-dimensional and can be implemented efficiently. However, section averaging is necessary to reduce the variance of the estimator. The averaging of M sections results in the following implementation:

$$B_g^{(M)}(u,v;0,0) = \frac{1}{M}\sum_{k=1}^{M} B_g^{(k)}(u,v;0,0) \tag{10}$$

where

$$\begin{aligned} B^{(k)}(u,v;0,0) &= G_k(u,v)G_k(0,0)G_k^*(u,v) \\ &= \left|G_k(u,v)\right|^2 G_k(0,0) \\ &= \left|H_k(u,v)F_k(u,v)+N_k(u,v)\right|^2\left[H_k(0,0)F_k(0,0)+N_k(0,0)\right] \end{aligned} \tag{11}$$

The expected value of $B_g^{(k)}(u,v;0,0)$ is proportional to the periodogram of the noise-free blurred image, if the noise is zero mean and the average of the original image is zero. The latter assumption does not hold in practice because images have non-negative values. Therefore, the original image average should be estimated and subtracted. When a good estimate of the original image mean value is obtained, and the number of sections M is large enough, the bispectrum can outperform the power spectrum.

3.2 The Bicepstrum

The bicepstrum is proposed as an alternative to the bispectrum for blur identification, similarly to the way the cepstrum may be used instead of the power spectrum. The power bicepstrum $D_g(p,q)$ is defined as

$$D_g(p,q) = \mathcal{F}^{-1}\left\{\log[B_g(u,v;0,0)]\right\} \tag{12}$$

The performance of the bicepstrum in the presence of noise is discussed in [14]. The bicepstrum utilizes the bispectrum and inherits robust performance in the presence of additive Gaussian noise. In addition, it provides all the advantages of cepstral analysis outlined in Section 2.3. As is the case with the power cepstrum, the bicepstrum can be postprocessed using the filter in (7). In the next section, simulation results using all of the above methods are presented.

4. RESULTS

The performance of the spectrum, cepstrum, bispectrum, and bicepstrum for the identification of linear motion blurs was experimentally investigated by simulations. The "cameraman" image was synthetically blurred using uniform linear motion PSF's of length 8 and 15 pixels. Gaussian noise was added to obtain SNR levels between 0 and 40 dB. The degraded image was divided in

500 one-dimensional sections, with 256 points in each section, and 128 point overlap between sections. The direction of scanning alternate rows in the image was reversed to preserve signal continuity. The 1-D data sections were windowed using a Hanning window. The first prominent local minimum of the power spectrum or the bispectrum was used to identify the first zero of the linear motion blur. The cepstrum and bicepstrum were computed based on the power spectrum and bispectrum respectively and were postprocessed using (7). The global maximum of the processed cepstrum or bicepstrum was used to identify the motion blur parameters. The simulation results showed that at SNR greater than 20 dB all methods performed well. In situations where the SNR was low and the blur size was small, the bispectrum outperformed the other methods. When the SNR was low and the blur was large, the bicepstrum provided the best results. Representative results are shown in Figures 1 through 4. It was determined that in most, but not all, cases postprocessing improved the performance of the cepstrum and the bicepstrum.

5. CONCLUSIONS

In this paper, the bicepstrum was employed as an alternative to the bispectrum for the identification of linear motion blur parameters. The biceptrum combines the advantages of cepstral analysis with the robustness of the bispectrum in the presence of additive Gaussian noise. However, for the bicepstrum to be effective averaging of large numbers of image sections is required. A comparative study of blur identification methods using spectral and higher-order spectral nulls was performed. At high SNR levels the performance of all methods is acceptable. At low SNR levels and large blurs the cepstrum and bicepstrum outperform the spectrum and bispectrum respectively. When the blur size is small and the SNR is low, the blur identification problem becomes very difficult and no single method consistently provides accurate PSF estimates.

6. ACKNOWLEDGMENTS

This work was supported in part by the NSF IUCRC Center for Electronic Imaging Systems

7. REFERENCES

[1] A. M. Tekalp, H. Kaufman, and J. W. Woods, "Identification of image and blur parameters in the restoration of noncausal blurs," *IEEE Trans. Acoust., Speech, Signal Proc.*, vol. 34, pp. 963-972, Aug. 1986.

[2] A. M. Tekalp and H. Kaufman, "On statistical identification of a class of linear space-invariant image blurs using non-minimum phase ARMA models," *IEEE Trans. Acoust., Speech, Signal Proc.*, vol. 36, pp. 1360-1363, Aug. 1988.

[3] R. L. Lagendijk, J. Biemond, and D. E. Boekee, "Identification and restoration of noisy blurred images using the expectation-maximization algorithm," *IEEE Trans. Acoust., Speech, Signal Proc.*, vol. 38, pp. 1180-1191, Jul. 1990.

[4] K. T. Lay and A. K. Katsaggelos, "Image identification and restoration based on the EM algorithm," *Optical Engineering*, vol. 29, May 1990.

[5] S. J. Reeves and R. M. Merserau, "Blur identification by the method of generalized cross-validation," *IEEE Trans. Image Proc.*, 1992.

[6] G. Pavlovic and A.M. Tekalp, "Maximum likelihood parametric blur identification based on a continuous spatial domain model," *IEEE Trans. Image Proc.*, vol 1, pp. 496-504, Oct. 1992.

[7] A. E. Savakis and H. J. Trussell, "Blur identification by residual spectral matching," *IEEE Trans. Image Proc.*, vol. 2, April 1993.

[8] D. B. Gennery, "Determination of optical transfer function by inspection of frequency-domain plot," *J. Opt. Soc. Amer.*, vol. 63, pp. 1571-1577, Dec. 1973.

[9] T. M. Cannon, "Blind deconvolution of spatially invariant image blurs with phase," *IEEE Trans. Acous., Speech, Signal Proc.*, vol. 24, pp. 58-63, Feb. 1976.

[10] M. M. Chang, A. M. Tekalp, A. T. Erdem, "Blur identification using the bispectrum," *IEEE Trans. Acous., Speech, Signal Proc.*, vol. 39, pp. 2323-2325, Oct. 1991.

[11] P. D. Welch, "The use of the fast Fourier transform for the estimation of power spectra," *IEEE Trans. Audio Electroacoust.*, vol. 15, pp. 70-73, Jun. 1967.

[12] R. Fabian and D. Malah, "Robust identification of motion and out-of-focus blur parameters from Blurred and Noisy Images," *CVGIP*, vol. 53, No. 5, pp. 403-412, Sept. 1991

[13] A. W. Lohmann and B. Wirnitzer, "Triple correlations," *Proceedings of the IEEE,* vol. 72, pp. 889-901, July 1984

[14] A. P. Petropulu and C. L. Nikias, "The complex cepstrum and bicepstrum: Analytic performance evaluation in the presence of Gaussian noise," *IEEE Trans. Acous., Speech, Signal Proc.*, vol. 38, pp. 1246-1256, July 1990

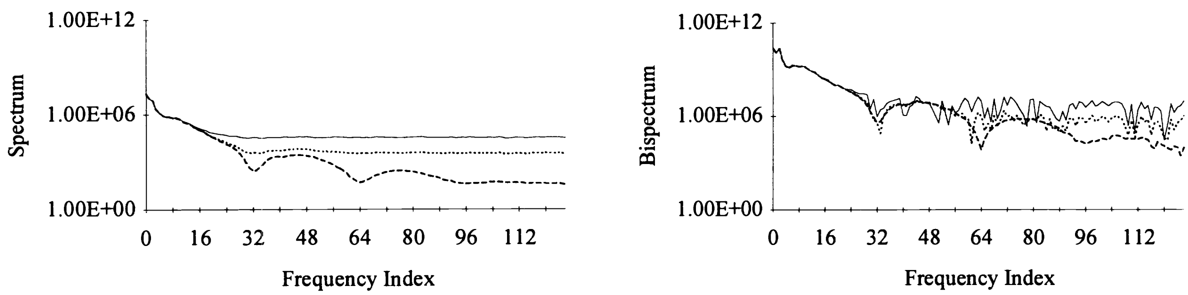

Figure 1: Spectrum and Bispectrum of "cameraman" image blurred with 8 pixel motion blur for SNR=40dB (broken line), SNR=20 dB (dotted line), and SNR=10dB (solid line)

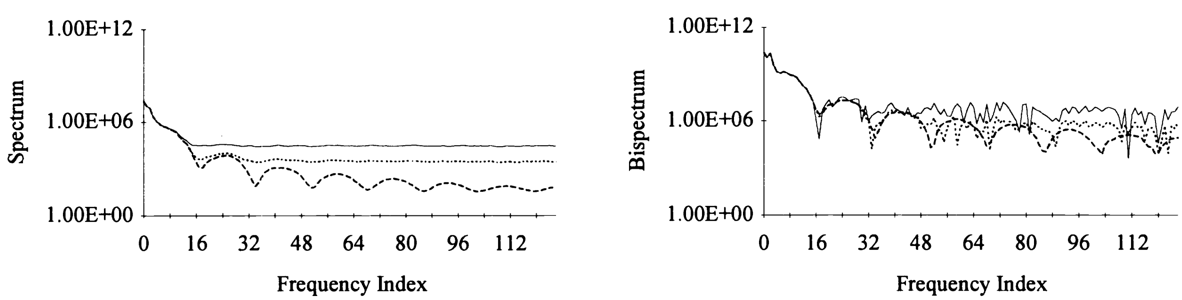

Figure 2: Spectrum and Bispectrum of "cameraman" image blurred with 15 pixel motion blur for SNR=40dB (broken line), SNR=20 dB (dotted line), and SNR=10dB (solid line)

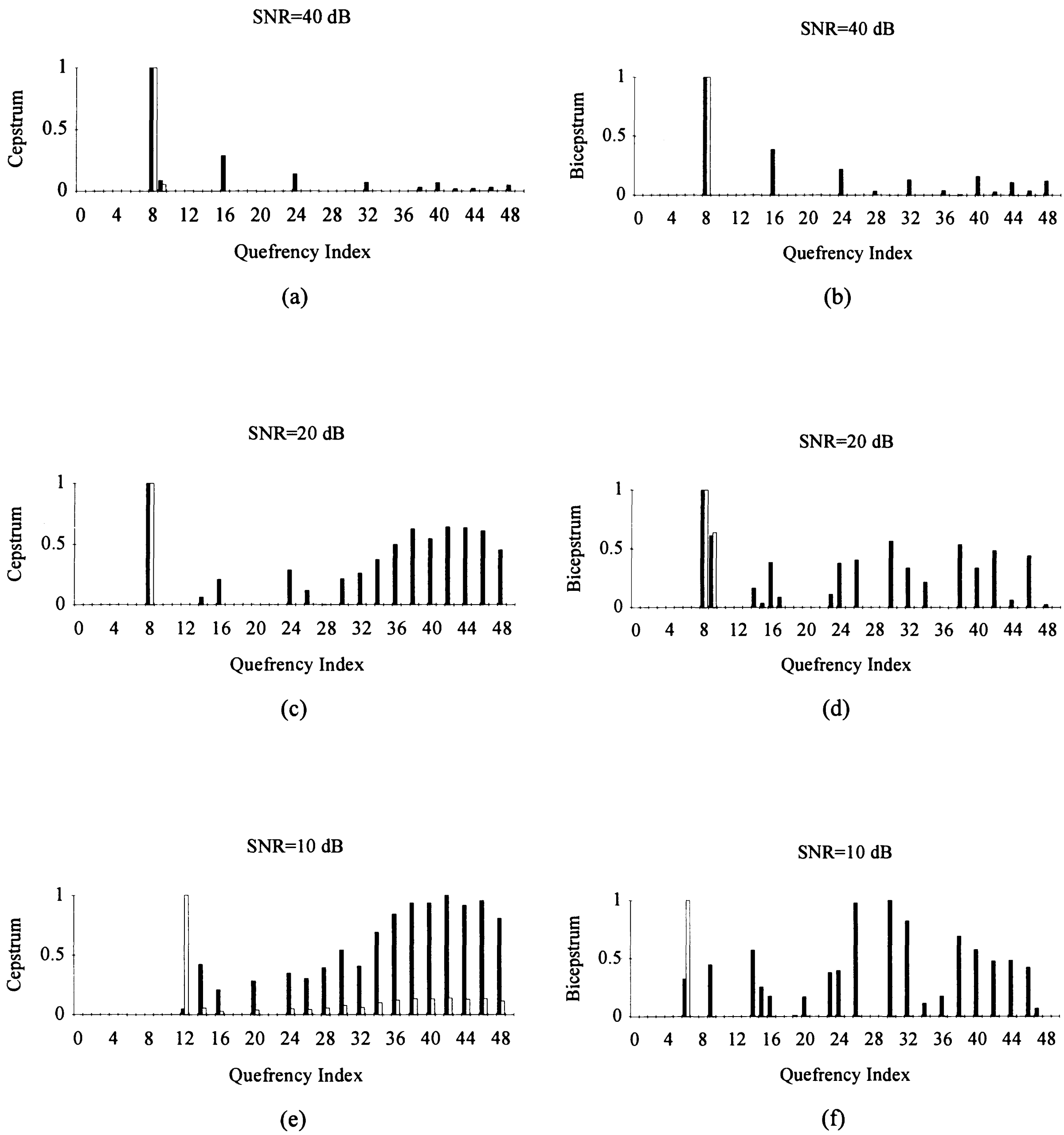

Figure 3: Cepstrum and Bicepstrum of "cameraman" image degraded with 8 pixel motion blur; signals were normalized by setting maximum to one; dark bars show the cepstrum or bicepstrum without postprocessing, light bars show the cepstrum or bicepstrum postprocessed using (7):
(a) Cepstrum at SNR=40dB, (b) Bicepstrum at SNR=40dB, (c) Cepstrum at SNR=20dB,
(d) Bicepstrum at SNR=20dB, (e) Cepstrum at SNR=10dB, (f) Bicepstrum at SNR=10dB

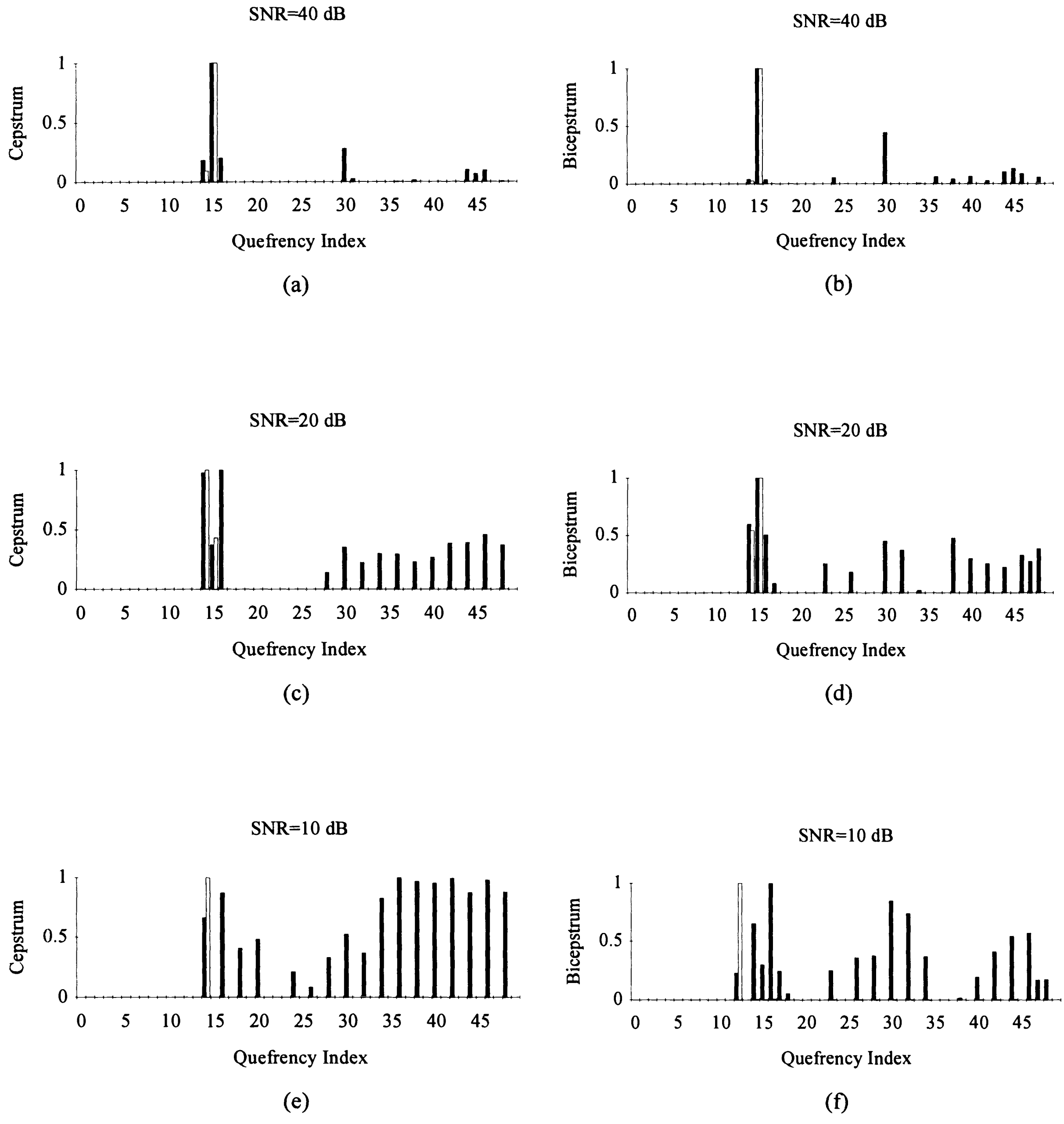

Figure 4: Cepstrum and Bicepstrum of "cameraman" image degraded with 15 pixel motion blur; signals were normalized by setting maximum to one; dark bars show the cepstrum or bicepstrum without postprocessing, light bars show the cepstrum or bicepstrum postprocessed using (7):
(a) Cepstrum at SNR=40dB, (b) Bicepstrum at SNR=40dB, (c) Cepstrum at SNR=20dB,
(d) Bicepstrum at SNR=20dB, (e) Cepstrum at SNR=10dB, (f) Bicepstrum at SNR=10dB